Published in final edited form as:
Heart Rhythm. 2014 August ; 11(8): 1446–1453. doi:10.1016/j.hrthm.2014.04.042.

Novel *SCN5A* Mutation in Amiodarone-responsive Multifocal Ventricular Ectopy-associated Cardiomyopathy

Thomas M. Beckermann, Ph.D.[1], **Karen McLeod, M.D.**[2], **Victoria Murday, M.D.**[2], **Franck Potet, Ph.D.**[3], and **Alfred. L. George Jr., M.D.**[1,3]

[1]Department of Pharmacology, Vanderbilt University, Nashville, Tennessee 37212 [2]Royal Hospital for Sick Children, Yorkhill, Glasgow G3 8SJ, Scotland UK [3]Division of Genetic Medicine, Department of Medicine, Vanderbilt University, Nashville, Tennessee 37212

Abstract

Background—Mutations in *SCN5A*, encoding the cardiac sodium channel ($Na_V1.5$) typically cause ventricular arrhythmia or conduction slowing. Recently, *SCN5A* mutations have been associated with heart failure combined with variable atrial and ventricular arrhythmia. Here we present the clinical, genetic and functional features of an amiodarone-responsive multifocal ventricular ectopy-related cardiomyopathy associated with a novel mutation in a $Na_V1.5$ voltage sensor domain.

Methods and results—A novel, *de novo SCN5A* mutation ($Na_V1.5$-R225P) was identified in a boy with prenatal arrhythmia and impaired cardiac contractility followed by postnatal multifocal ventricular ectopy suppressible by amiodarone. We investigated the functional consequences of $Na_V1.5$-R225P expressed heterologously in tsA201 cells. Mutant channels exhibited significant abnormalities in both activation and inactivation leading to large, hyperpolarized window- and ramp-currents that predict aberrant sodium influx at potentials near the cardiomyocyte resting membrane potential. Mutant channels also exhibited significantly increased persistent (late) sodium current. This profile of channel dysfunction shares features with other *SCN5A* voltage sensor mutations associated with cardiomyopathy and overlapped that of congenital long-QT syndrome. Amiodarone stabilized fast inactivation, suppressed persistent sodium current and enhanced frequency-dependent rundown of channel availability.

Conclusion—We determined the functional consequences and pharmacological responses of a novel *SCN5A* mutation associated with an arrhythmia-associated cardiomyopathy. Comparisons with other cardiomyopathy-associated $Na_V1.5$ voltage sensor mutations revealed a pattern of abnormal voltage dependence of activation as a shared molecular mechanism of the syndrome.

Address for Correspondence: Alfred L. George, Jr., M.D., Department of Pharmacology, Northwestern University Feinberg School of Medicine, Searle 8-510, 320 East Superior Street, Chicago, IL 60611, Tel: 312-503-4892, al.george@northwestern.edu.

Conflicts of interest: The authors have no disclosures.

Keywords

SCN5A mutation; cardiomyopathy; electrophysiology; amiodarone

INTRODUCTION

The voltage-gated cardiac sodium channel $Na_V1.5$ encoded by *SCN5A* is responsible for the initial upstroke of the cardiac action potential.[1] Mutations in *SCN5A* typically manifest as cardiac arrhythmias such as the congenital long-QT or Brugada syndromes, or by variable degrees of impaired cardiac conduction. Importantly, some *SCN5A* mutations are associated with clinical features that overlap more than one disorder.[2] Additionally, a new genotype-phenotype correlation has emerged recently that has expanded the clinical spectrum of sodium channelopathies to include disorders which feature impaired cardiac contractility.

In 2004, McNair *et al*. described a multigenerational family segregating *SCN5A*-D1275N with a complex disorder featuring variable combinations of supraventricular arrhythmias, impaired atrioventricular conduction and dilated cardiomyopathy.[3] Shortly thereafter, Olson *et al*. screened a cohort of patients diagnosed with idiopathic dilated cardiomyopathy and identified five *SCN5A* mutations including a novel voltage sensor mutation (R814W).[4] Subsequent functional studies of R814W revealed a novel pattern of sodium channel dysfunction featuring a prominent defect in the voltage-dependence of activation.[5] Two other SCN5A voltage sensor mutations associated with cardiomyopathy and variable arrhythmias have been identified (R219H, R222Q).[6–11] The R222Q mutation exhibits many of the same biophysical abnormalities as R814W, whereas R219H appears to have a distinct functional perturbation (gating pore leak current). Importantly, the clinical syndrome associated with some of these mutations, best illustrated for R222Q, exhibits reversibility of contractile dysfunction with antiarrhythmic therapy.[7] However, the pharmacological mechanism responsible for this effect has not been explored. Here, we present a novel *SCN5A* mutation ($Na_V1.5$-R225P) associated with prenatal arrhythmias, impaired cardiac contractility, and postnatal multifocal ventricular ectopy-associated ventricular dysfunction reversed by amiodarone treatment. We elucidated the functional consequences of the mutation and demonstrated the likely mechanism for amiodarone efficacy. These findings extend the phenotypic spectrum of *SCN5A* mutations and reveal a plausible pharmacological mechanism underlying the reversibility of arrhythmia-associated cardiomyopathy.

METHODS

Subject Ascertainment

The mother of the proband volunteered her son’s clinical history and genetic information without solicitation. Subsequently, informed consent was obtained to evaluate medical record information including genetic testing data. The informed consent procedure was approved by the Vanderbilt University Institutional Review Board. Genetic testing for mutations in *KCNQ1*, *KCNH2*, *SCN5A*, *KCNE1*, *KCNE2* and *KCNJ2* was performed by The Scottish Genetics Laboratory, Aberdeen.

Cloning and expression of $Na_V1.5$

A cDNA encoding human $Na_V1.5$ was cloned into the bicistronic vector pRc-CMV_IRES2-CD8 and mutations were created using site-directed mutagenesis. Human-derived tsA201 cells (HEK293 cell line expressing SV40 large T antigen) were transiently transfected with 1.0 μg of WT or mutant $Na_V1.5$ plasmid using FuGeneHD (Roche Diagnostics, Indianapolis, IN) in combination with 0.6 μg of a bicistronic plasmid (pIRES-EGFP-hβ1) encoding enhanced green fluorescent protein (GFP) and the human β1 subunit (hβ1) under the control of the CMV immediate early promoter. Positively transfected cells were determined by GFP emission and the binding of beads conjugated with anti-CD8 antibodies.

Electrophysiology

Sodium currents were recorded at room temperature (22–23°C) 48–72 hours after transfection using the whole-cell patch clamp technique as previously described.[5] All data were analyzed using pCLAMP 10.0 or Microsoft Excel 2007 and plotted using SigmaPlot 10.0 (Systat Software, Inc., San Jose, CA). Statistical analysis was performed using Student's t-Test.

Experiments examining persistent I_{Na} and ramp-currents utilized tetrodotoxin (TTX; Tocris Bioscience, Bristol, UK) to allow for the determination of TTX-sensitive sodium current. TTX was added to the bath solution from a stock solution of TTX (3 mM in water) to a final concentration of 30 μM. TTX-sensitive current was determined by offline digital subtraction.

Pharmacology

Amiodarone hydrochloride (Sigma-Aldrich, St. Louis, MO) was dissolved in dimethyl sulfoxide (DMSO; Sigma-Aldrich) to create a stock concentration of 30 mM. For experiments, amiodarone stock was diluted into bath solution for use at 3 μM concentration. Fresh dilutions were made on the day of experiments. Amiodarone or DMSO was continually present in the superfusate during experiments examining the biophysical effects of amiodarone. DMSO concentration never exceeded 0.01% in control or test conditions.

RESULTS

Case Presentation

A Caucasian male was delivered at 37 weeks gestation following an eventful 15 week antenatal course. Fetal tachycardia accompanied by poor ventricular function was noted at 22 weeks. Maternal flecainide administration was initiated at 27 weeks. At 28 weeks, fetal tachycardia with 2:1 atrioventricular (AV) conduction was noted and suggested a supraventricular origin of the arrhythmia. Tachycardia persisted despite escalating the dosage of flecainide. Propranolol was added at 31 weeks and fetal heart rate normalized with concomitant improvement in ventricular function. A maternal flecainide/propranolol regimen was maintained through parturition.

Immediately following birth, a wandering atrial rhythm at 137 bpm with frequent, multifocal ventricular ectopic beats was noted (Fig. 1A, Supplemental Fig. S1A). Treatment with

amiodarone (5 mg/kg initially three times daily for one week, then twice daily for one week followed by a maintenance dose of amiodarone 5 mg/kg daily) in combination with propranolol (1 mg/kg four times daily; 3 mg four times daily absolute dose) was initiated. Continued atrial and ventricular ectopy was evident at age 1 month, and an ECG obtained at 7 weeks showed atrial tachycardia (atrial rate 260 bpm) with 2:1 AV block (Fig. 1B, Fig. S1B). The antiarrhythmic regimen was not changed. By 3 months of age, an ECG was reported as showing predominantly sinus rhythm with some ectopy (trace not available). Because of persistent sinus rhythm at age 6 months, amiodarone was discontinued while propranolol was continued (3 mg four times daily). Two weeks after stopping amiodarone, an ECG showed sinus rhythm but with a prolonged QTc interval of 480 msec (Fig. 1C, Fig. S1C). Propranolol was discontinued at that time. However, he was hospitalized 6 weeks later with supraventricular tachycardia (200 bpm) and multifocal ventricular ectopy (Fig. 1D, Fig. S1D) Echocardiography demonstrated impaired ventricular function (ejection fraction 43%, fractional shortening 17%; Fig. S2). Amiodarone was restarted with an initial loading dose followed by a maintenance dose of 5 mg/kg/day. Propranolol was reinstituted at a dose of 1 mg/kg four times daily and he was started on captopril 0.5 mg/kg three times daily. This regimen suppressed abnormal rhythms (Fig. 1E, Fig. S1E) and there was improvement in ventricular function albeit with an unexplained change in P wave morphology as compared to age 6.5 months (Fig. 1C). Subsequent attempts to replace amiodarone with sotalol were unsuccessful with recurrence of tachycardia, increased frequency of ventricular ectopy and one episode of nonsustained ventricular tachycardia. There were no documented episodes of ventricular arrhythmia that resembled torsades de pointes. At age 6 years, the proband remained on amiodarone but propranolol was substituted with nadolol. There have been rare syncopal events, no occurrences of cardiac arrest, but mild growth retardation was noted. Invasive electrophysiological testing was not performed.

There is no family history of cardiac arrhythmia or sudden unexplained death. Both parents and an older female sibling are healthy with normal heart rhythms and normal ECG indices including normal QTc intervals. Genetic testing of the proband revealed a novel missense mutation in *SCN5A* predicting the substitution of arginine at position 225 with proline (R225P). Neither parent nor the sibling carried this variant, consistent with a *de novo* mutation in the proband.

Functional properties of $Na_V1.5$-R225P

We compared the functional properties of WT and R225P mutant cardiac sodium channels ($Na_V1.5$) heterologously expressed in tsA201 cells with the human β_1 subunit (Fig. 2). Cells expressing R225P exhibited significantly greater current density and appeared to activate at more hyperpolarized potentials than WT channels (Fig. 2A,B). Boltzmann fits of the conductance-voltage plots revealed similar voltage dependence of activation for WT and R225P ($V_{½}$ values: WT, −37.3±0.06 mV; R225P, −37.1±1.0) but R225P exhibited a significantly shallower slope (WT: 8.4±0.2, R225P: 12.3±0.3; $p<0.005$; Fig. 2C; Supplemental Table S1) suggesting a blunted voltage sensitivity. Activation kinetics, as determined by the time-to-peak current at an activating potential of −20mV, were also significantly altered in the mutant channel (R225P: 0.96±0.01 ms; WT: 0.67±0.02 ms;

p<0.005; Fig. S3A; Table S1). These findings were consistent with a structural perturbation of the domain 1 voltage-sensor segment that disrupts channel activation.

In addition to abnormalities in activation, inactivation of R225P channels was also abnormal (Fig. 2D). Time constants for inactivation determined by fitting current decay with a double exponential function were significantly larger for R225P channels across a range of voltages compared to WT channels indicating slower inactivation (Fig. 2E). Additionally, the mutant channels exhibited a significantly larger fraction of current inactivating with a slow component (time constant τ_2; Fig. S3B). Cells expressing R225P also had a significantly larger persistent current measured as a percentage of peak current (0.87±0.06%, n=10) compared to WT channels (0.13±0.02%, n=18; p<0.005; Fig. 2F; Table S1). This level of increased persistent current was similar to what we observed in parallel experiments for an LQTS-associated mutant $Na_V1.5$ channel (delKPQ: 0.65±0.04%, n=8; Table S1).[12] By contrast, the voltage dependence of steady-state inactivation (channel availability) and the time course of recovery from fast inactivation of R225P were not overtly different from WT channels (Fig. S3C,D; Table S1). Although the voltage midpoints ($V_{½}$ values) for activation and inactivation were not affected by the mutation, the more shallow activation curve slope caused a significantly expanded ‘window current’ defined as the extent of overlap between the two curves (Fig. 3A). This suggests that the R225P mutation could evoke aberrant sodium current activation at voltages within the window.

The potential for aberrant sodium current activation was further probed by examining channel responses to depolarizing voltage ramps. Comparing R225P ramp-currents to those of WT channels revealed critical differences in magnitude and kinetics. For R225P, averaged ramp currents exhibit activation with a broad, nearly bifid peak at significantly more hyperpolarized potentials than WT channels (Fig. 3B; Table S1). Net charge movement during voltage ramps was 8-fold greater for R225P than WT channels (WT: 0.66±0.1 pC/nA, R225P: 5.86±0.6 pC/nA; p<0.005) (Fig. S4; Table S1). These findings indicate that aberrant sodium current conducted by R225P channels can be evoked by voltages close to the resting membrane potential of cardiomyocytes.

Altered slow inactivation of R225P channels

To further investigate the functional consequences of R225P, we examined the sensitivity of the mutant channel to frequency-dependent rundown. Stimulating at 2 Hz with a 5 ms test pulse, we did not identify a difference in current amplitude between WT and R225P following 100 pulses (Fig. 4A, Fig. S5; Table S2). However, at pulse lengths of 100 ms and 300 ms, there was a significant divergent in current amplitude for WT and R225P at pulse 100, with the mutant channel exhibiting a greater sensitivity to the rundown protocol. This dependence on the pulse duration without an overt difference in recovery from fast inactivation suggested possible involvement of enhanced slow inactivation to explain the greater activity-dependent loss of channel availability observed for R225P.

We compared the slow inactivation properties of WT and R225P channels. As illustrated by Fig. 4B and data in Table S2, both WT and R225P channels enter slow inactivation with similar rates during conditioning pulses up to 3000 ms. However, for conditioning pulse durations longer than 3000 ms, the behavior of WT and R225P channels diverge, with

R225P showing enhanced entry into a slow inactivated state. Using a 3000 ms test pulse (approximate midpoint for onset of slow inactivation for both WT and R225P), we measured recovery from slow inactivation (Fig. 4C, Table S2). The biexponential time course of recovery from slow inactivation observed for R225P was significantly slower than WT channels. Further, we observed that the voltage-dependence of slow inactivation was significantly shifted in the hyperpolarized direction for R225P compared with WT channels (Fig. 4D, Table S2). Collectively, these findings indicate that the R225P mutation stabilizes the slow inactivated state and enhances the tendency for slow inactivation. To determine whether this enhanced slow inactivation might affect the ramp current, we examined channel availability following a series of ramp depolarizations (500 ms ramps; 1.1 Hz). There was a significant decrease in charge movement at pulse 100 for R225P but not WT channels. Despite this effect of repetitive pulsing, charge movement associated with voltage ramps remained greater for R225P than WT channels (Fig. S4B; Table S2).

Comparisons with other SCN5A mutations

Two other mutations have been identified previously affecting the same residue as R225P, but the associated clinical phenotypes and functional disturbances are different. Mutation R225Q was identified in a heterozygous subject exhibiting a mild form of LQTS without reported features of cardiomyopathy.[13] We characterized $Na_V1.5$-R225Q. (Fig. S6; Table S1) and found rather minor differences in channel activation and channel availability (hyperpolarized shifts) compared with WT channels. We also observed an increased persistent current (Table S1) although ramp currents did not differ with that of WT channels. Mutation R225W was identified in a heterozygous woman without symptoms, but also in her child with severe conduction disturbances who had a second mutation (W156X) inherited from the father.[14] Functional studies of the R225W mutation demonstrated a positively shifted channel availability curve and a significant decrease in current density, distinct from the constellation of findings we observed for R225P.

By contrast, the functional properties of R225P channels resembled features of two other *SCN5A* mutations identified in subjects diagnosed with either dilated cardiomyopathy (R814W)[4, 5] or multifocal ventricular ectopy with reversible contractile dysfunction (R222Q).[7, 11] Mutation R222Q affects another conserved arginine residue in the D1/S4 voltage sensor segment and is located approximately one helix turn away from position 225. The R814W mutation also alters a conserved voltage sensor arginine residue but in the second domain. We compared biophysical properties of R222Q and R814W and found that both mutations exhibit altered conductance-voltage relationships and predispose channels to activation at more hyperpolarized potentials during slow voltage ramps similar to R225P (Fig. 5; Fig. S7). In contrast to R225P, neither R222Q nor R814W exhibited increased persistent sodium current (Table S1).

A comparison of normalized ramp currents for these three mutants with that of a representative LQTS mutation (delKPQ) reveals an interesting segregation of the voltage range in which the currents peak (Fig. 5; Table S1). Specifically, those mutations clinically associated with impaired ventricular function peak at more hyperpolarized potentials than the LQTS mutation. Additionally, average ramp currents exhibited by R225P are nearly

bifid with one component peaking around −70 mV (similar to R222Q and R814W) while the second component peaks near −40 mV, closer to delKPQ. We deduced that the hyperpolarized activation of R222Q, R814W and the main component of R225P ramp currents correlated with the altered activation voltage dependence, whereas the more depolarized activation observed for delKPQ and the second component of R225P are associated with increased persistent sodium current and a slower time course of fast inactivation. Finally, both R814W[5] and R225P exhibit similar enhanced slow inactivation properties, but R222Q was not previously tested in this manner.

Amiodarone effects on R225P

Because the proband responded to treatment with amiodarone, we compared the pharmacological effects of this drug on WT and mutant channels (Fig. 6; Fig. S8; Table S3). For both WT and R225P, amiodarone (3 μM) slowed activation kinetics (Fig. S8B), and significantly altered voltage-dependence of inactivation (Fig. 6A) and recovery from inactivation (Fig. 6C). Additionally, the drug had mutant-specific effects including suppression of persistent sodium current (Fig. S8C; Table S3) and a hyperpolarized shift in the conductance-voltage relationship (Fig. 6A) resulting in an accentuated window current. Interestingly, amiodarone did not alter the peak ramp current density, but caused a significant decrease in charge movement determined for R225P channels (Fig. 6B). The effect of amiodarone to slow recovery from inactivation for both WT and R225P channels likely explains a profound reduction in channel availability during pulse trains (Fig. 6D; Table S3) and a decrease in charge movement observed in repetitive ramp experiments (Fig. S8D; Table S3). The suppression of channel availability most likely dominates the effects of amiodarone on $Na_V1.5$ and may account for the suppression of ventricular ectopy in the proband.

DISCUSSION

We present functional and pharmacological studies of a novel mutation in the principal cardiac voltage-gated sodium channel associated with multifocal ventricular ectopy with reversible ventricular dysfunction. Our data provide a biophysical profile of the mutant channel and examine pharmacological mechanisms responsible for the favorable clinical response to amiodarone. The novel mutation, R225P, adds to the growing structural and functional diversity of mutations in *SCN5A* responsible for inherited arrhythmia susceptibility and highlights the unique phenotype associated with mutations in first and second domain voltage sensors.

Phenotypes associated with *SCN5A* voltage sensor mutations

The mutation $Na_V1.5$-R225P alters a critical arginine residue located in the voltage sensing S4 segment of the first domain (D1), one of the structures involved with detecting changes in membrane potential. Three previously identified *SCN5A* mutations associated with cardiomyopathy also affect critical arginine residues within the D1/S4 (R219H, R222Q) or D2/S4 (R814W) segments and are associated with complex clinical phenotypes featuring atrial and ventricular arrhythmias, and cardiomyopathy.[6–11] By contrast, missense mutations replacing S4 segment arginine residues in D4 cause congenital long-QT syndrome without

contractile dysfunction.[15–17] This intriguing genotype-phenotype divergence may stem from differences in the contributions of the various voltage sensing segments and how mutations within each domain affect sodium channel gating.[18] Importantly, the two other mutations identified at position $Na_V1.5$-R225 (R225W, R225Q) are associated with different clinical phenotypes and, correspondingly, different functional disturbances.

The association of arrhythmia and cardiomyopathy with voltage sensor mutations was originally reported in 2005 by Olson and colleagues. A *de novo* D2/S4 mutation (R814W) was identified in a young woman who had dilated cardiomyopathy combined with atrial flutter and nonsustained ventricular tachycardia.[4] Our laboratory later demonstrated that this mutation causes prominent defects in the kinetics and voltage dependence of activation that promoted aberrant activation during slow voltage ramps.[5] A similar functional defect was subsequently observed for the D1/S4 mutation R222Q, which had been identified independently by four groups. The phenotype associated with R222Q was described variably as peripartum dilated cardiomyopathy,[6,19] arrhythmic dilated cardiomyopathy,[9] escape capture bigeminy and cardiomyopathy,[10] reversible ventricular ectopy and dilated cardiomyopathy or multifocal ectopic Purkinje-related premature contractions.[7] Most of these reports emphasized the high burden of ectopic premature ventricular beats and impaired cardiac contractility with the variable presence of atrial tachyarrhythmias.

Pathophysiological implications

Given that three of the D1/S4 and D2/S4 mutations have common patterns of dysfunction, most notable for altered activation voltage dependence, a shared pathophysiology would be logical to assume. One demonstrable consequence of altered activation is aberrant sodium conductance at hyperpolarized potentials during voltage ramps. This *in vitro* phenomenon suggests that mutant sodium channels could produce an aberrant inward current at near resting membrane potentials of cardiac myocytes. This would promote enhanced automaticity and may specifically trigger ventricular extrasystoles arising ectopically from Purkinje fibers as suggested by computer modeling studies.[7,11] A high burden of ectopic beats may lead to heart failure that can be reversed by pharmacological suppression of sodium current as was noted in our case and previous reports of R222Q. However, this same functional defect could possibly induce contractile dysfunction through disordered calcium handling,[20] improper pH regulation,[21] or disrupted mitochondrial function[22,23] that might not be reversible. Interestingly, another D1/S4 mutation (R219H) associated with dilated cardiomyopathy and ventricular arrhythmia causes a novel type of sodium channel dysfunction (proton leak current) that could also disrupt intracellular pH regulation in myocytes.[8]

Unlike the previously characterized $Na_V1.5$ voltage sensor mutations discussed above, ramp-currents produced by R225P propagate in two distinct sets of peaks. The first peak can be attributed to the large, hyperpolarized window current of the mutant channel, as seen with R814W and R222Q, while the second peak is a result of the persistent current produced by R225P, similar to the LQTS mutation delKPQ.[12] This interesting characteristic has been previously discussed in relation to the neuronal sodium channel $Na_V1.3$ in which biphasic peaks were attributed to window- and persistent currents respectively.[24] Consistent with

observations made with other *SCN5A* mutations associated with LQTS,[12] R225P exhibits increased persistent current and this may explain the prolonged QTc observed in the proband.

Mechanism of amiodarone response

Because amiodarone was successful in suppressing ventricular ectopy and restoring normal contractile function, we sought to determine the pharmacological effects of this drug on the mutant sodium channel. We found that amiodarone significantly suppressed persistent current recorded from cells expressing R225P, induced a slightly hyperpolarized increase in window-current, and changed the overall morphology of the ramp-current resulting in a decreased charge movement for the mutant channel. In addition, amiodarone also had a profound impact on recovery from inactivation that suggested a mechanism for dampening the deleterious biophysical dysfunction of R225P. Specifically, by prolonging recovery time from fast inactivation, amiodarone effectively diminished the pool of available mutant channels. Further, frequency-dependent rundown of channels in the presence of amiodarone was greater for R225P than WT channels. Because R225P is more sensitive to inactivation induced rundown, we predict that amiodarone administration results in a global decrease in the total number of channels available to be activated, however, the proportion of WT channels in the population is enriched compared to R225P.

Conclusions

We identified a novel *de novo SCN5A* mutation in a child with an amiodarone-responsive multifocal ventricular ectopy-associated cardiomyopathy and elucidated the molecular mechanism responsible for the disorder. The mutation, R225P, affects a voltage sensor domain and causes a hyperpolarized shift in the voltage dependence of activation. Additionally, this mutation evokes increased persistent sodium current, a recognized biophysical defect underlying type 3 LQTS, and other biophysical abnormalities including enhanced slow inactivation. Amiodarone suppresses channel availability to a greater extent for the mutant and attenuates the aberrant ramp current, two plausible explanations for its therapeutic success in this case. The unique functional consequences of *SCN5A* voltage sensor mutations in D1 and D2 help explain the pathogenesis of an arrhythmia-associated cardiomyopathy that can be reversed with certain sodium channel blocking drugs.

Supplementary Material

Refer to Web version on PubMed Central for supplementary material.

Acknowledgments

The authors are grateful to the participating family. We thank Drs. Prince Kannankeril, Katherine Murray, Stacy Killen and Dan Roden for helpful advice.

FUNDING SOURCES

This work was supported by NIH grant HL083374 (A.L.G.) and by a Scientist Development Grant (11SDG5330006) from the American Heart Association (F.P.).

Abbreviations

LQTS	long-QT syndrome
TTX	tetrodotoxin
AV	atrioventricular
GFP	green fluorescent protein
DMSO	dimethyl sulfoxide

References

1. George AL Jr. Molecular and genetic basis of sudden cardiac death. J Clin Invest. 2013; 123:75–83. [PubMed: 23281413]
2. George, AL, Jr. Mechanisms in heritable sodium channel diseases. In: Zipes, DP.; Jalife, J., editors. Cardiac Electrophysiology: From Cell to Bedside. 6. Philadelphia: Elsevier; 2013.
3. McNair WP, Ku L, Taylor MR, et al. SCN5A mutation associated with dilated cardiomyopathy, conduction disorder, and arrhythmia. Circulation. 2004; 110:2163–2167. [PubMed: 15466643]
4. Olson TM, Michels VV, Ballew JD, et al. Sodium channel mutations and susceptibility to heart failure and atrial fibrillation. JAMA. 2005; 293:447–454. [PubMed: 15671429]
5. Nguyen TP, Wang DW, Rhodes TH, George AL Jr. Divergent biophysical defects caused by mutant sodium channels in dilated cardiomyopathy with arrhythmia. Circ Res. 2008; 102:364–371. [PubMed: 18048769]
6. Morales A, Painter T, Li R, et al. Rare variant mutations in pregnancy-associated or peripartum cardiomyopathy. Circulation. 2010; 121:2176–2182. [PubMed: 20458009]
7. Laurent G, Saal S, Amarouch MY, et al. Multifocal Ectopic Purkinje-Related Premature Contractions: A New SCN5A-Related Cardiac Channelopathy. J Am Coll Cardiol. 2012; 60:144–156. [PubMed: 22766342]
8. Gosselin-Badaroudine P, Keller DI, Huang H, et al. A Proton Leak Current through the Cardiac Sodium Channel Is Linked to Mixed Arrhythmia and the Dilated Cardiomyopathy Phenotype. PLoS ONE. 2012; 7:e38331. [PubMed: 22675453]
9. McNair WP, Sinagra G, Taylor MR, et al. SCN5A Mutations Associate With Arrhythmic Dilated Cardiomyopathy and Commonly Localize to the Voltage-Sensing Mechanism. J Am Coll Cardiol. 2011; 57:2160–2168. [PubMed: 21596231]
10. Nair K, Pekhletski R, Harris L, et al. Escape Capture Bigeminy: Phenotypic Marker of Cardiac Sodium Channel Voltage Sensor Mutation R222Q. Heart Rhythm. 2012; 9:1681–1688. [PubMed: 22710484]
11. Mann SA, Castro ML, Ohanian M, et al. R222Q SCN5A mutation is associated with reversible ventricular ectopy and dilated cardiomyopathy. J Am Coll Cardiol. 2012; 60:1566–1573. [PubMed: 22999724]
12. Bennett PB, Yazawa K, Makita N, George AL Jr. Molecular mechanism for an inherited cardiac arrhythmia. Nature. 1995; 376:683–685. [PubMed: 7651517]
13. Millat G, Chevalier P, Restier-Miron L, et al. Spectrum of pathogenic mutations and associated polymorphisms in a cohort of 44 unrelated patients with long QT syndrome. Clin Genet. 2006; 70:214–227. [PubMed: 16922724]
14. Bezzina CR, Rook MB, Groenewegen WA, et al. Compound heterozygosity for mutations (W156X and R225W) in SCN5A associated with severe cardiac conduction disturbances and degenerative changes in the conduction system. Circ Res. 2003; 92:159–168. [PubMed: 12574143]
15. Kambouris NG, Nuss HB, Johns DC, et al. Phenotypic characterization of a novel long-QT syndrome mutation (R1623Q) in the cardiac sodium channel. Circulation. 1998; 97:640–644. [PubMed: 9495298]

16. Makita N, Shirai N, Nagashima M, et al. A de novo missense mutation of human cardiac Na^+ channel exhibiting novel molecular mechanisms of long QT syndrome. FEBS Lett. 1998; 423:5–9. [PubMed: 9506831]

17. Wang DW, Yazawa K, George AL Jr, Bennett PB. Characterization of human cardiac Na^+ channel mutations in the congenital long QT syndrome. Proc Natl Acad Sci USA. 1996; 93:13200–13205. [PubMed: 8917568]

18. Cha A, Ruben PC, George AL Jr, Fujimoto E, Bezanilla F. Voltage sensors in domains III and IV, but not I and II, are immobilized by Na^+ channel fast inactivation [see comments]. Neuron. 1999; 22:73–87. [PubMed: 10027291]

19. Cheng J, Morales A, Siegfried JD, et al. SCN5A rare variants in familial dilated cardiomyopathy decrease peak sodium current depending on the common polymorphism H558R and common splice variant Q1077del. Clin Transl Sci. 2010; 3:287–294. [PubMed: 21167004]

20. Bers DM, Barry WH, Despa S. Intracellular Na^+ regulation in cardiac myocytes. Cardiovasc Res. 2003; 57:897–912. [PubMed: 12650868]

21. Pieske B, Houser SR. $[Na^+]_i$ handling in the failing human heart. Cardiovasc Res. 2003; 57:874–886. [PubMed: 12650866]

22. Maack C, Cortassa S, Aon MA, et al. Elevated cytosolic Na^+ decreases mitochondrial Ca^{2+} uptake during excitation-contraction coupling and impairs energetic adaptation in cardiac myocytes. Circ Res. 2006; 99:172–182. [PubMed: 16778127]

23. Kohlhaas M, Liu T, Knopp A, et al. Elevated cytosolic Na^+ increases mitochondrial formation of reactive oxygen species in failing cardiac myocytes. Circulation. 2010; 121:1606–1613. [PubMed: 20351235]

24. Estacion M, Waxman SG. The response of $Na_V1.3$ sodium channels to ramp stimuli: multiple components and mechanisms. J Neurophysiol. 2013; 109:306–314. [PubMed: 23114218]

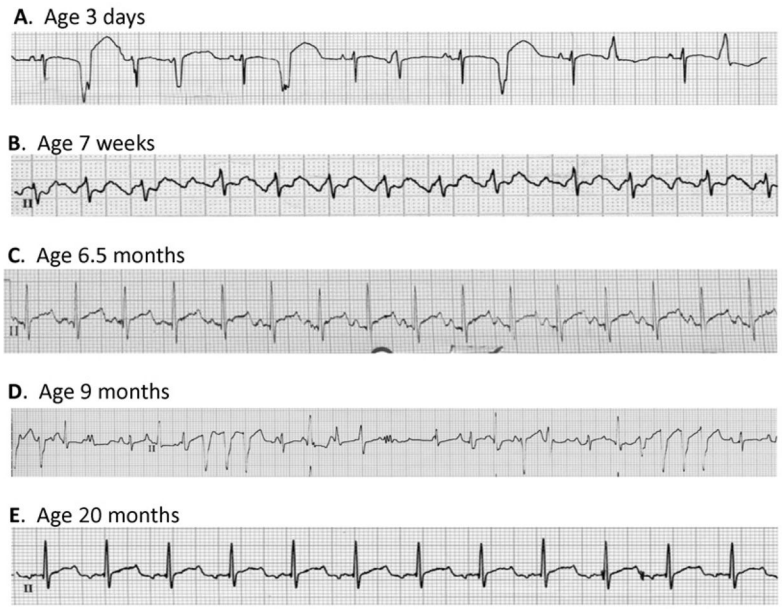

Figure 1. Electrocardiograms from the proband

(A) Representative lead II recording obtained at age 3 days illustrating wandering atrial rhythm with frequent multifocal premature ventricular beats. (B) Representative lead II recording obtained at age 7 weeks illustrating an episode of supraventricular tachycardia with variable 2:1 and 3:1 AV block. (C) Representative lead II recording obtained at age 6.5 months two weeks off amiodarone illustrating sinus rhythm with a prolonged QTc (480 ms). (D) Representative lead II recording obtained at age 9 months while the proband was off antiarrhythmic drugs illustrating multifocal ventricular ectopy and two 3–4 beat runs of nonsustained ventricular tachycardia. (E) Representative lead II recording obtained at age 20 months while treated with amiodarone and propranolol illustrating sinus rhythm. More complete ECG recordings corresponding to each of these events are provided as Supplemental Fig. S2.

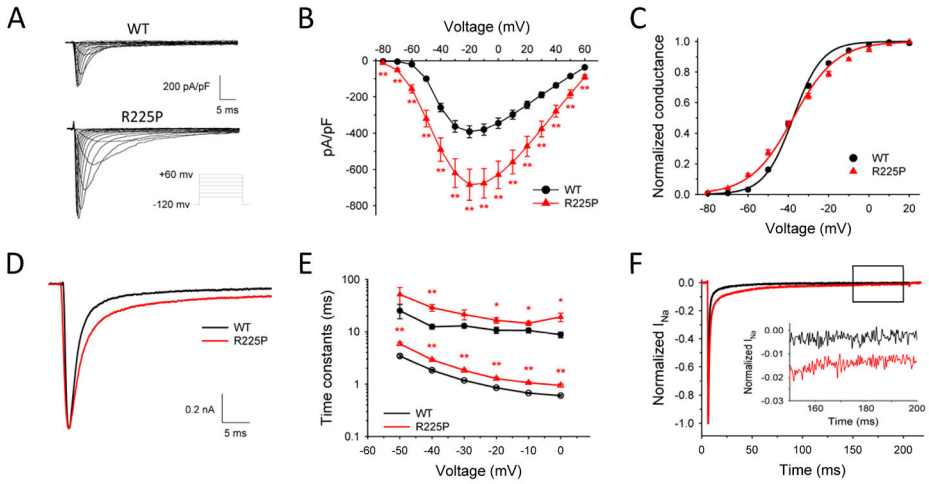

Figure 2. Biophysical properties of R225P

Biophysical properties of $Na_V1.5$-R225P. (A) Representative traces of WT (top) and R225P (bottom) sodium channels. (B) Current-density/voltage plots of WT and R225P. (C) Voltage dependence of activation for WT and R225P from −80 to +20 mV. (D) Representative traces of WT and R225P illustrating altered activation and inactivation kinetics. (E) Voltage-dependence of inactivation time constants (open symbols represent fast component; closed symbols represent slow component) for WT and R225P. (F) Representative TTX-subtracted whole cell current for WT and R225P. Persistent current was measured over the final 10 ms of a 200 ms pulse to −20 mV and normalized to peak current. Inset shows persistent current over the final 50 ms. All data are represented as mean ± S.E.M for n=11–18 cells.

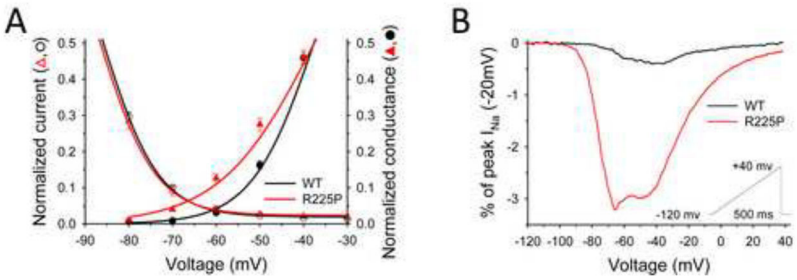

Figure 3. Window- and Ramp-currents

Window and ramp-currents of $Na_V1.5$-R225P reveal aberrant I_{Na} at hyperpolarized potentials. (A) Overlay of Boltzmann-fitted G/V and channel availability curves of WT and R225P emphasizing window-currents. (B) Normalized TTX-subtracted average ramp-currents (0.32 mV/ms) of WT and R225P measured as a percentage of peak I_{Na} (−20mV). All data are represented as mean ± S.E.M for n=7–15 cells.

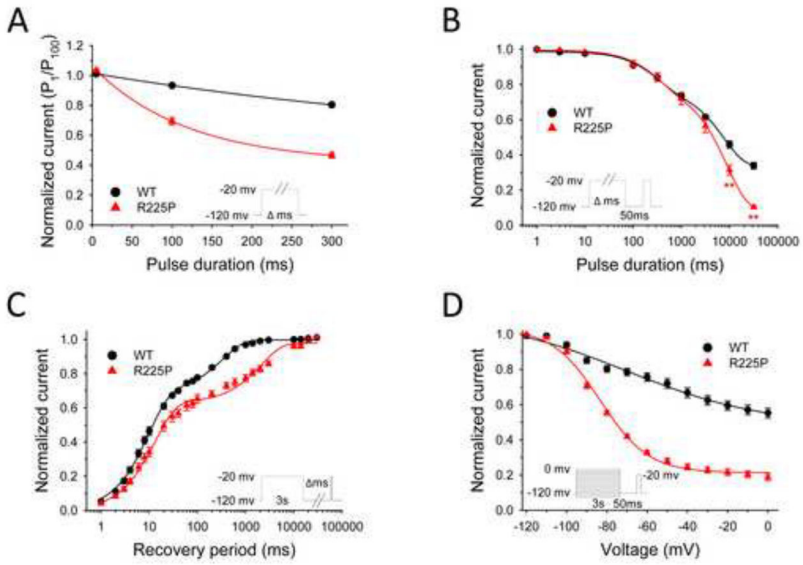

Figure 4. Frequency-dependent channel rundown and slow inactivation

$Na_V1.5$-R225P stabilizes the slow-inactivated state. (A) Frequency-dependent channel rundown of WT (black) and R225P (red) observed for activating pulse durations of 5, 100, and 300 ms. Curves were fit with exponential decay functions. (B) Onset of slow inactivation for WT and R225P. (C) Recovery from slow inactivation. WT (black line) and R225P (red line) data fit with double-exponential curves. (D) Voltage-dependence of slow-inactivation of WT and R225P. Curves are the result of data fittings with the Boltzmann function. All data are represented as mean ± S.E.M for n=7–15 cells.

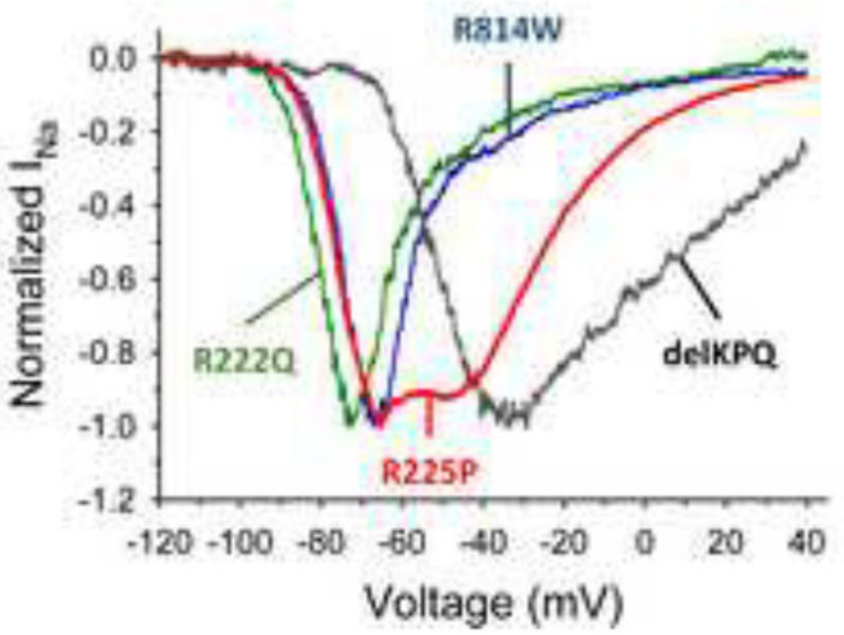

Figure 5. Normalized ramp-currents

Comparison of normalized ramp-currents. Normalized TTX-subtracted averaged ramp-currents from R225P and other $Na_V1.5$ mutations associated with multifocal ventricular ectopy with impaired cardiac contractility (R222Q), sporadic dilated cardiomyopathy (R814W), and congenital long-QT syndrome (delKPQ). All data are represented as mean for n=7–15 cells.

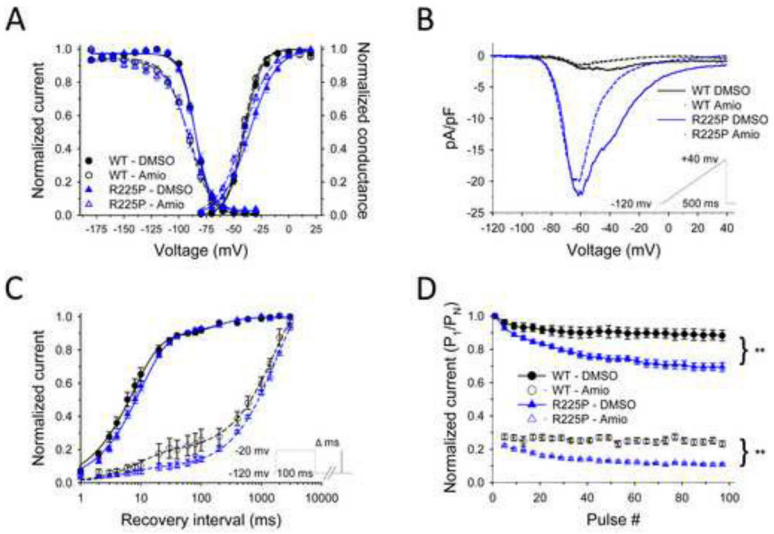

Figure 6. Biophysical properties of R225P in the presence of Amiodarone (3 μM)

Effects of amiodarone on $Na_V1.5$-R225P. (A) Activation and channel availability properties of WT and R225P in the presence of amiodarone (open symbols, dashed lines) or DMSO (filled circles, solid lines). All data were fit with a Boltzmann function. (B) TTX-subtracted averaged ramp-currents (0.32 mV/ms) of WT and R225P normalized to cell capacitance in the presence of amiodarone (dashed lines) or DMSO (solid lines). (C) Recovery from fast inactivation of WT and R225P in the presence of amiodarone (open symbols, dashed lines) or DMSO (filled circles, solid lines). The data were fit with a double exponential curve. (D) Pulse trains (2Hz; −20mV) with an activating pulse of 100ms of WT and R225P channels in the presence of amiodarone (open symbols, dashed lines) or DMSO (filled circles, solid lines). All data are represented as mean ± S.E.M for n=5–12 cells.